

The Kondo effect in the presence of the Rashba spin-orbit interaction

Rok Žitko, Janez Bonča

Jožef Stefan Institute, Jamova 39, SI-1000 Ljubljana, Slovenia,

Faculty of Mathematics and Physics, University of Ljubljana, Jadranska 19, SI-1000 Ljubljana, Slovenia

(Dated: October 6, 2018)

We study the temperature scale of the Kondo screening of a magnetic impurity which hybridizes with a two-dimensional electron gas in the presence of the Rashba spin-orbit interaction. The problem is mapped to an effective single-band impurity model with a hybridization function having an inverse-square-root divergence at the bottom of the band. We study the effect of this divergence on the Kondo screening. The problem is solved numerically without further approximations using the numerical renormalization group technique. We find that the Rashba interaction leads to a small variation of the Kondo temperature (increase or decrease) which depends on the values of the impurity parameters.

PACS numbers: 71.70.Ej, 72.10.Fk, 73.20.At

The spin-orbit (SO) interaction is a relativistic effect due to the inter-dependence between electric and magnetic fields when considered from different reference frames. It leads to a coupling between electron's spin and its (orbital) motion in real space¹. The effect is stronger in heavy elements from the bottom of the periodic system. The spin-orbit interaction plays a central role in many proposals for spintronic devices² and it is the physical origin of the recently discovered topologically non-trivial insulator phases which do not break the time-reversal symmetry³⁻⁶. The spin-orbit interaction does not break the Kramers degeneracy, thus the Kondo screening of magnetic moments is possible⁷⁻⁹ and should be observable in magnetic adatoms on topological insulator surfaces or on thin layers of heavy elements¹⁰.

The Kondo effect due to magnetic impurities in bulk simple metals was shown to be strongly suppressed by doping the host material with small amounts of Pt impurities which have a large value of the SO coupling constant¹¹, although these results have been questioned and the expected trend with the increasing strength of the SO coupling has not been confirmed in later experiments¹². An Anderson impurity model with SO scattering term for the conduction band electrons was studied by performing a Schrieffer-Wolff transformation into an effective Kondo model¹³ and it captured some (but not all) of the observations of Ref. 11. Kondo screening has also been studied through weak-localization effects; the results indicate that adding spin-orbit scatterers does not change the magnetic scattering at all^{7,14}. It was pointed out that the spin-orbit scatterers play the same role as elastic nonmagnetic impurities because they do not break the time-reversal symmetry⁷, thus the Kondo temperature is expected to remain unchanged, in agreement with the experiment. For similar reason of time-reversal invariance, the Kondo screening of magnetic moments is expected to occur for magnetic impurities adsorbed on the surfaces of three-dimensional topological insulators^{8,9}, unless the doping level is sufficiently high for the spontaneous breaking of the time-reversal symmetry due to magnetic ordering. The effect of the spin-orbit coupling in a two-dimensional (2D) electron gas with Rashba interaction¹ on the Kondo screening has been studied in Ref. 15. The work was based on a Kondo impurity Hamiltonian and after considering to which conduction-band

angular modes the impurity spin couples to, a two-channel Kondo model was derived, in which each channel has a different dispersion relation. By expanding the dispersion relations to linear order, remarking that the Fermi velocity is the same in both helicity channels, and after some further manipulations, the model maps to a single-channel single-impurity Kondo model with unchanged dimensionless Kondo coupling constant ρJ . In other words, it was predicted that turning on the Rashba coupling (all other parameters remaining the same) does not change the Kondo temperature at all, except perhaps for some effective band-width effects. The same problem has been considered starting from an Anderson impurity model and using the Varma-Yafet variational ansatz¹⁶; this work did not specifically address the question of the Kondo temperature beyond noting that it remains constant in the limit of small Rashba coupling, but focused instead on the spatial distribution of the spin correlations. Recently, a new study of this system used a Schrieffer-Wolff transformation to obtain an effective two-channel Kondo model with an additional Dzyaloshinsky-Moriya (DM) interaction¹⁷. Using a scaling renormalization group analysis, it was argued that the DM term renormalizes the Kondo coupling and produces an exponential enhancement of the Kondo temperature. This effect has not been observed in previous studies. Since all the cited works are based on various mappings and approximations, it is unclear which result for the variation of the Kondo temperature (or lack thereof) is correct and what approximations are responsible for the disagreement. For this reason, we reexamine the problem using an approach where all the approximations are well controlled. To wit, we integrate out the conduction-band degrees of freedom to obtain an impurity action with a hybridization function which has an inverse-square-root-divergence at the bottom of the conduction band. This step is exact. We then numerically study the effective impurity model using the numerical renormalization group (NRG) method^{18,19}. While the NRG approach is not exact, the approximations involved are all well controlled. We find that the Kondo temperature is only weakly affected by the Rashba interaction: it may weakly (approximately linearly) increase or decrease depending on the values of the impurity parameters.

We study a magnetic impurity embedded in the 2D electron

gas with Rashba spin-orbit interaction^{1,15–17,20}. The impurity is described using the single-orbital Anderson impurity model H_0 with an additional Rashba interaction term H_{SO} :

$$H_0 = \epsilon(n_\uparrow + n_\downarrow) + Un_\uparrow n_\downarrow \quad (1)$$

$$+ \sum_{\mathbf{k}\sigma} \epsilon_k c_{\mathbf{k}\sigma}^\dagger c_{\mathbf{k}\sigma} + \sum_{\mathbf{k}\sigma} V_k \left(c_{\mathbf{k}\sigma}^\dagger d_\sigma + \text{H.c.} \right), \quad (2)$$

$$H_{SO} = \alpha \sum_{\mathbf{k}} \psi_{\mathbf{k}}^\dagger (k_x \sigma_y - k_y \sigma_x) \psi_{\mathbf{k}} \quad (3)$$

$$= \alpha \sum_{\mathbf{k}} k e^{-i\phi_{\mathbf{k}}} c_{\mathbf{k}\uparrow}^\dagger c_{\mathbf{k}\downarrow} + \text{H.c.} \quad (4)$$

The operator d_σ^\dagger creates an electron in the impurity level, while $c_{\mathbf{k}\sigma}^\dagger$ correspond to the conduction-band electrons with the dispersion $\epsilon_k = k^2/2m^* + E_0$, where \mathbf{k} is the crystal momentum, m^* the effective electron mass, and E_0 the bottom of the conduction band. The occupancy operator is $n_\sigma = d_\sigma^\dagger d_\sigma$. The chemical potential is set to the energy zero, $\mu = 0$. In H_{SO} , α parametrizes the strength of the Rashba spin-orbit interaction, $\psi_{\mathbf{k}}$ is a spinor field $\{c_{\mathbf{k}\uparrow}, c_{\mathbf{k}\downarrow}\}^T$, while $\sigma_{x/y}$ are Pauli matrices. k and $\phi_{\mathbf{k}}$ are the polar coordinates of the wave number \mathbf{k} , with the polar axis oriented along k_y .

We now switch to a continuum representation in a box of volume $\mathcal{V} \equiv 1$. The sums are transformed in the standard way as $\sum_{\mathbf{k}} \rightarrow \mathcal{V}/(2\pi)^2 \int k dk d\phi$. The operators are transformed as $c_{\mathbf{k}\sigma} \rightarrow (2\pi/\mathcal{V}) \psi_{\mathbf{k}\sigma}^\dagger$; they are normalized such that $\{\psi_{\mathbf{k}\sigma}, \psi_{\mathbf{k}'\sigma'}^\dagger\} = \delta^{(2)}(\mathbf{k} - \mathbf{k}') \delta_{\sigma\sigma'}$. Noting that $\delta^{(2)}(\mathbf{k}) = \delta(k)\delta(\phi)/k$, we switch to a polar representation using $\psi_{\mathbf{k}\sigma} \rightarrow 1/\sqrt{k} \xi_{k\phi\sigma}$, with $\{\xi_{k\phi\sigma}, \xi_{k'\phi'\sigma'}^\dagger\} = \delta(k - k') \delta(\phi - \phi') \delta_{\sigma\sigma'}$. Finally, we switch to the angular momentum basis $\xi_{k\phi\sigma} = \frac{1}{\sqrt{2\pi}} \sum_m e^{im\phi} c_{k\sigma}^m$, where m is the orbital magnetic quantum number^{8,15,17} and the anticommutation relations take the form $\{c_{k\sigma}^m, (c_{k'\sigma'}^m)^\dagger\} = \delta(k - k') \delta_{mm'} \delta_{\sigma\sigma'}$. Collectively, these transformation steps can be written as

$$c_{\mathbf{k}\sigma} \rightarrow \sqrt{\frac{2\pi}{k}} \sum_{m=-\infty}^{\infty} e^{im\phi} c_{k\sigma}^m. \quad (5)$$

We then introduce the linear combination which diagonalizes the conduction-band Hamiltonian including the Rashba coupling terms^{15,17}

$$c_{kh}^{m+1/2} = \left(c_{k\uparrow}^m + h c_{k\downarrow}^{m+1} \right) / \sqrt{2}, \quad (6)$$

where $h = \pm 1$ is the chirality quantum number. The corresponding band energies are

$$\epsilon_{kh} = \epsilon_k + \alpha kh = \frac{(k + hk_0)^2}{2m^*} + E_0 - E_R, \quad (7)$$

where $k_0 = m^* \alpha$ is the Rashba momentum, and $E_R = k_0^2/2m^*$ is the Rashba energy. This implies that the bottom of the conduction band shifts from E_0 to $E_0 - E_R$ upon switching on the Rashba interaction.

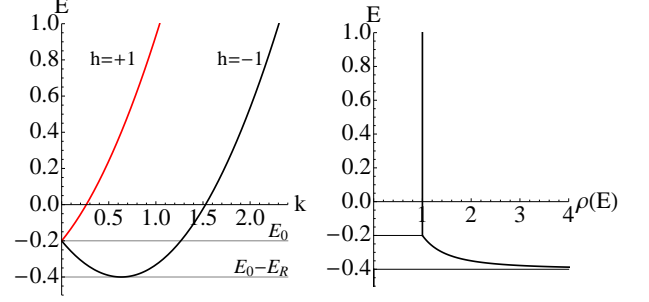


Figure 1: (Color online) The dispersion and the density of states in the presence of the Rashba spin-orbit coupling. The label $h = \pm 1$ indicates the helicity of the band.

We obtain the effective impurity model

$$H = \sum_{hm} \int_0^\infty dk \epsilon_{kh} \left(c_{kh}^{m+1/2} \right)^\dagger c_{kh}^{m+1/2} + \epsilon(n_\uparrow + n_\downarrow) + Un_\uparrow n_\downarrow + \frac{1}{2\pi} \sum_h \int_0^\infty \sqrt{k} dk V_k \frac{\sqrt{2\pi}}{\sqrt{2}} \times \left[\left(c_{kh}^{1/2} \right)^\dagger d_\uparrow + (-1)^{\frac{h-1}{2}} \left(c_{kh}^{-1/2} \right)^\dagger d_\downarrow + \text{H.c.} \right]. \quad (8)$$

We now integrate out the conduction-band modes and obtain an effective impurity action of the following form:

$$S = \int_0^\beta d\tau \left[\sum_\sigma d_\sigma^\dagger \left(\frac{\partial}{\partial \tau} + \epsilon \right) d_\sigma + Un_\uparrow n_\downarrow \right] + \frac{1}{\pi} \sum_h \int_0^\beta d\tau \int_0^\beta d\tau' d_\sigma^\dagger \Delta_h(\tau - \tau') d_\sigma. \quad (9)$$

The hybridization function $\Delta_h(\tau)$ is the Fourier transform of

$$\Delta_h(i\omega_n) = \frac{1}{4\pi} \int_0^\infty k dk \frac{V_k^2}{i\omega_n - \epsilon_{kh}}. \quad (10)$$

While $\Delta_+(i\omega_n)$ and $\Delta_-(i\omega_n)$ are somewhat complicated functions, their sum $\Delta = \sum_h \Delta_h$ is simple. Assuming $V_k \equiv V$, the imaginary part $\Gamma(E) = -1/(2\pi) \text{Im} \Delta(E + i0^+)$ is found to be of the same functional form as the density of states (DOS) of the conduction band:

$$\Gamma(E) = \Gamma_0 \begin{cases} 0 & E < E_0 - E_R \\ \sqrt{\frac{E_R}{E - (E_0 - E_R)}} & E_0 - E_R < E < E_0 \\ 1 & E > E_0 \end{cases} \quad (11)$$

where $\Gamma_0 = \pi \frac{m^*}{2\pi} V^2$. This result is remarkably simple and could have been guessed in advance, since the impurity is assumed to be point-like and simply couples to the local DOS at its position. The only effect of the Rashba interaction as

far as the local impurity properties are concerned is the emergence of an additional energy interval $[E_0 - E_R; E_0]$ with finite density of states which diverges with an inverse-square-root divergence at the lower limit, see Fig. 1. The effect of this diverging density of states is difficult to evaluate analytically, therefore we resort to using a numerical technique.

We compute the impurity spectral function using the numerical renormalization group (NRG) method^{18,19} with extensions for arbitrary density of states²¹⁻²⁸. NRG can handle diverging DOS both at the Fermi level^{25,29}, as well as away from the Fermi level³⁰. Here the discretization has been performed using the discretization scheme from Refs. 27,28; this scheme easily handles inverse square root divergencies at finite frequencies without a need for introducing artificial cut-offs. NRG parameters were $\Lambda = 2$, twist-averaging over $N_z = 64$ discretization grids, and the truncation cutoff set at $10\omega_N$, where ω_N is the characteristic energy scale at the N -th NRG step.

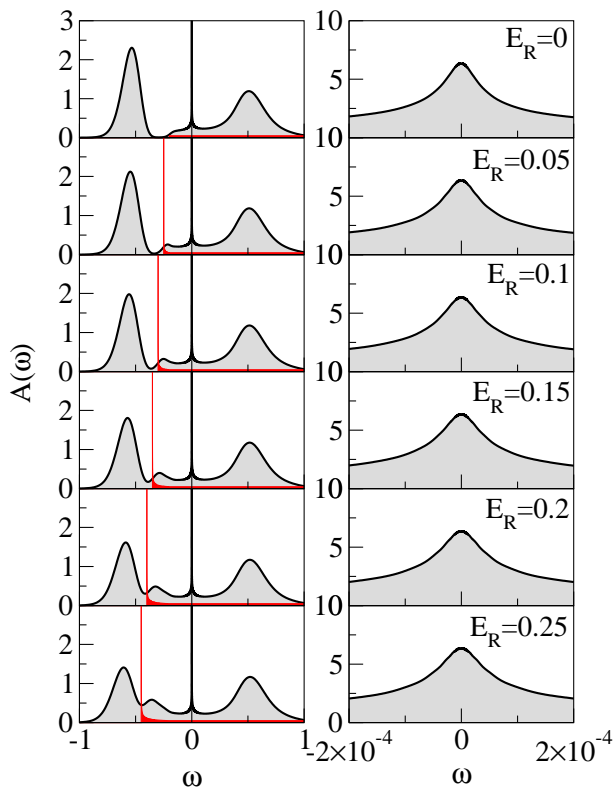


Figure 2: (Color online) The impurity spectral functions for a range of the Rashba spin-orbit coupling strengths. The gray curve (red online) in the left-hand panels is the effective hybridization function that the impurity state mixes with. The parameters are $U = 1$, $\epsilon = -0.5$, and the hybridization strength at Fermi level for $E_R = 0$ has been set to $\Gamma_0 = 0.05$. The band bottom is $E_0 = -0.2$.

The calculated spectral functions are shown in Fig. 2. Left panels show the spectral function over the full energy interval, while the right panels are a close-up on the Kondo resonance at the Fermi level. The hybridization function entering the impurity model is shown as a gray curve (red online) in the left-hand panels. The spectral function features two atomic

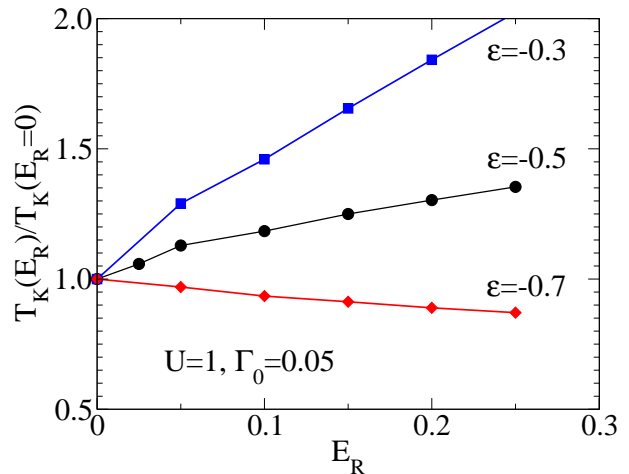


Figure 3: (Color online) The Kondo temperature calculated using the NRG. The parameters are specified in the plot. The temperatures are rescaled by the Kondo temperature in the absence of the Rashba interaction.

resonances, one at $\omega = \epsilon$ (corresponding to the extraction of an electron) and one at $\omega = \epsilon + U$ (corresponding to the addition of an electron). The width of atomic spectral peaks is approximately $2\Gamma(\omega)$, where ω is the peak position^{31,32}. The peak at $\omega = \epsilon$ lies outside the band for all values of E_R considered, thus it should have zero width (i.e., it is a delta peak); the finite width in the presented spectral functions is due to the spectral broadening in the NRG. In addition to the atomic peaks, the spectral function features the many-body Kondo resonance which peaks near the Fermi level. The long logarithmic tails of the Kondo resonance are asymmetric due to the particular energy dependence of the hybridization function. At the bottom of the band, at $\omega = E_0 - E_R$, the spectral function has a maximum, then it drops to zero at lower frequencies since in that range there are no states in the band. Again, the drop to zero in presented spectral functions is overbroadened due to technical reasons.

The Kondo temperature (defined as in Ref. 33) has been determined from the impurity magnetic susceptibility, but it could alternatively be extracted from the Kondo resonance peak widths. The results for a several different choices of the impurity parameters are shown in Fig. 3. Note that we have included parameter sets both with $\epsilon + U/2 = 0$ and with $\epsilon + U/2 \neq 0$. We find that the Kondo temperature exhibits some variation as a function of E_R , however the variation is not exponential¹⁷, but rather linear in the large- E_R limit with more complex variation for small values of E_R (which can be attributed to the emergence of the inverse-square-root divergence in the hybridization function). Depending on the value of ϵ , U , and Γ_0 , the Kondo temperature is either an increasing or a decreasing function of E_R .

In systems with constant hybridization function Γ , the Kondo temperature is given approximately by

$$T_K = \tilde{D}\sqrt{\rho J} \exp\left(-\frac{1}{\rho J}\right), \quad (12)$$

where $\rho J = 8\Gamma/\pi U$ is the dimensionless Kondo coupling constant. If the hybridization function is energy-dependent, we have to use its value at the Fermi level (Γ_0) in the expression above. In the presence of the Rashba interaction, if the bottom of the conduction band is initially below the Fermi level (i.e., $E_0 < 0$), the density of states at $\omega = 0$ will remain unchanged when the Rashba coupling is increased. This explains the absence of an exponential renormalization of T_K and is in agreement with Ref. 15. Nevertheless, in Eq. (12) the effective bandwidth \tilde{D} does depend on the details of the hybridization function, thus some variation of T_K is in fact expected and indeed observed, as shown in Fig. 3.

We note that the effective impurity action, Eq. (9), has the form of a single-band problem. In fact, the single-orbital Anderson impurity model is always effectively a single-band problem, no matter what kind of conduction-band it couples to^{8,24}. The required unique effective conduction band can always be constructed by taking the combination of states which couples to the impurity orbital (here a state proportional to the linear combination $\sum_{\mathbf{k}} V_k c_{\mathbf{k}\sigma}^\dagger$) as an initial state in the Gram-Schmidt orthogonalization procedure applied on the conduction-band Hamiltonian. Consequently, one obtains a single-band tight-binding Hamiltonian, while all other conduction-band states are fully decoupled from the impurity. This argument holds universally. A multi-channel Kondo model can be in some cases obtained from the single-orbital Anderson impurity model by using a non-optimal basis for the conduction-band modes that also includes states which are in reality fully decoupled from the impurity. These states

should not in any way affect impurity properties. Unfortunately, the complete irrelevance of the redundant conduction-band states can only be observed if the problem is solved exactly. If the problem is, however, approached with an approximate method, there exist a potential pitfall: the presence of the redundant states can affect the impurity properties in some spurious way.

We also note that the problem of an impurity in the two-dimensional electron gas can never be truly particle-hole symmetric, because the conduction-band itself is not particle-hole symmetric. We therefore do not expect any particular difference in the role of the Rashba spin-orbit interaction depending on whether $\epsilon + U/2$ is zero or not¹⁷.

The predictions of this work could be experimentally tested in a system where the spin-orbit interaction can be tuned, such as 2D electron systems in semiconductors with metal gates. Furthermore, the rapid advances in the field of ultra-cold atom system suggest that it might become possible to build 2D fermionic gases with tunable SO interaction³⁴⁻³⁷ and couple it to a magnetic impurity³⁸.

Acknowledgments

Discussions with Anton Ramšak and Tomaž Rejec and the support of the Slovenian Research Agency (ARRS) under Program P1-0044 are acknowledged.

-
- ¹ R. Winkler, *Spin-orbit coupling effects in two-dimensional electron and hole systems* (Springer-Verlag, 2003).
- ² I. Žutić, J. Fabian, and S. D. Sarma, *Rev. Mod. Phys.* **76**, 323 (2004).
- ³ C. L. Kane and E. J. Mele, *Phys. Rev. Lett.* **95**, 146802 (2005).
- ⁴ B. A. Bernevig, T. L. Hughes, and S. C. Zhang, *Science* **314**, 1757 (2006).
- ⁵ M. König et al., *Science* **318**, 766 (2007).
- ⁶ L. Fu and C. L. Kane, *Phys. Rev. B* **76**, 045302 (2007).
- ⁷ Y. Meir and N. S. Wingreen, *Phys. Rev. B* **50**, 4947 (1994).
- ⁸ R. Žitko, *Phys. Rev. B* **81**, 241414(R) (2010).
- ⁹ X.-Y. Feng, W.-Q. Chen, J.-H. Gao, Q.-H. Wang, and F.-C. Zhang, *Phys. Rev. B* **81**, 235411 (2010).
- ¹⁰ C. R. Ast, G. Wittich, P. Wahl, R. Vogelgesang, D. Pacilé, M. C. Falub, L. Moreschini, M. Papagno, M. Grioni, and K. Kern, *Phys. Rev. B* **75**, 201401(R) (2007).
- ¹¹ D. Gainon and A. J. Heeger, *Phys. Rev. Lett.* **22**, 1420 (1969).
- ¹² M. Bujatti, D. Wohlleben, and M. B. Maple, *Phys. Rev. B* **13**, 3984 (1976).
- ¹³ B. Giovannini, *Phys. Rev. B* **3**, 870 (1971).
- ¹⁴ G. Bergmann, *Phys. Rev. Lett.* **57**, 1460 (1986).
- ¹⁵ J. Malecki, *J. Stat. Phys.* **129**, 741 (2007).
- ¹⁶ X.-Y. Feng and F.-C. Zhang, *J. Phys.: Condens. Matter* **23**, 105602 (2011).
- ¹⁷ M. Zarea, S. E. Ulloa, and N. Sandler, *Enhancement of the kondo effect through rashba spin-orbit interaction*, arxiv:1105.3522 (2011).
- ¹⁸ K. G. Wilson, *Rev. Mod. Phys.* **47**, 773 (1975).
- ¹⁹ R. Bulla, T. Costi, and T. Pruschke, *Rev. Mod. Phys.* **80**, 395 (2008).
- ²⁰ Y. A. Bychkov and E. I. Rashba, *J. Phys. C: Solid State Phys.* **17**, 6039 (1984).
- ²¹ W. C. Oliveira and L. N. Oliveira, *Phys. Rev. B* **49**, 11986 (1994).
- ²² K. Chen and C. Jayaprakash, *Phys. Rev. B* **52**, 14436 (1995).
- ²³ K. Ingersent, *Phys. Rev. B* **54**, 11936 (1996).
- ²⁴ R. Bulla, T. Pruschke, and A. C. Hewson, *J. Phys.: Condens. Matter* **9**, 10463 (1997).
- ²⁵ M. Vojta and R. Bulla, *Eur. Phys. J. B* **28**, 283 (2002).
- ²⁶ V. L. Campo and L. N. Oliveira, *Phys. Rev. B* **72**, 104432 (2005).
- ²⁷ R. Žitko and T. Pruschke, *Phys. Rev. B* **79**, 085106 (2009).
- ²⁸ R. Žitko, *Comp. Phys. Comm.* **180**, 1271 (2009).
- ²⁹ R. Žitko, J. Bonča, and T. Pruschke, *Phys. Rev. B* **80**, 245112 (2009).
- ³⁰ R. Peters and T. Pruschke, *Phys. Rev. B* **79**, 045108 (2009).
- ³¹ T. Pruschke and N. Grewe, *Z. Phys. B* **74**, 439 (1989).
- ³² D. E. Logan, M. P. Eastwood, and M. A. Tusch, *J. Phys.: Condens. Matter* **10**, 2673 (1998).
- ³³ H. R. Krishna-murthy, J. W. Wilkins, and K. G. Wilson, *Phys. Rev. B* **21**, 1003 (1980).
- ³⁴ X.-J. Liu, M. F. Borunda, X. Liu, and J. Sinova, *Phys. Rev. Lett.* **102**, 046402 (2009).
- ³⁵ J. Dalibard, F. Gerbier, G. Juzeliunas, and P. Öhberg, *Colloquium: Artificial gauge potentials for neutral atoms*, arxiv:1008.5378 (2010).
- ³⁶ Y.-J. Lin, K. Jiménez-García, and I. B. Spielman, *Nature* **471**, 83 (2011).

³⁷ M. Chapman and C. Sá de Melo, *Nature* **471**, 41 (2011).

³⁸ A. Recati, P. O. Fedichev, W. Zwerger, J. von Delft, and P. Zoller,

Phys. Rev. Lett. **94**, 040404 (2005).